EWI-2 Association with α-Actinin Regulates T Cell Immune Synapses and HIV Viral Infection

Mónica Gordón-Alonso, Mónica Sala-Valdés, Vera Rocha-Perugini, Daniel Pérez-Hernández, Soraya López-Martín, Angeles Ursa, Susana Álvarez, Tatiana V. Kolesnikova, Jesús Vázquez, Francisco Sánchez-Madrid and María Yáñez-Mó

J Immunol 2012; 189:689-700; Prepublished online 11 June 2012;
doi: 10.4049/jimmunol.1103708
http://www.jimmunol.org/content/189/2/689

The Journal of Immunology is published twice each month by
The American Association of Immunologists, Inc.,
9650 Rockville Pike, Bethesda, MD 20814-3994.

Print ISSN: 0022-1767 Online ISSN: 1550-6606.

EWI-2 Association with α-Actinin Regulates T Cell Immune Synapses and HIV Viral Infection

Mónica Gordón-Alonso,*[,1] Mónica Sala-Valdés,[†,1] Vera Rocha-Perugini,[†] Daniel Pérez-Hernández,[‡] Soraya López-Martín,[§] Angeles Ursa,* Susana Álvarez,[¶] Tatiana V. Kolesnikova,[‖] Jesús Vázquez,[‡] Francisco Sánchez-Madrid,*[,†] and María Yáñez-Mó[§]

EWI motif-containing protein 2 (EWI-2) is a member of the Ig superfamily that links tetraspanin-enriched microdomains to the actin cytoskeleton. We found that EWI-2 colocalizes with CD3 and CD81 at the central supramolecular activation cluster of the T cell immune synapse. Silencing of the endogenous expression or overexpression of a cytoplasmic truncated mutant of EWI-2 in T cells increases IL-2 secretion upon Ag stimulation. Mass spectrometry experiments of pull-downs with the C-term intracellular domain of EWI-2 revealed the specific association of EWI-2 with the actin-binding protein α-actinin; this association was regulated by PIP2. α-Actinin regulates the immune synapse formation and is required for efficient T cell activation. We extended these observations to virological synapses induced by HIV and found that silencing of either EWI-2 or α-actinin-4 increased cell infectivity. Our data suggest that the EWI-2–α-actinin complex is involved in the regulation of the actin cytoskeleton at T cell immune and virological synapses, providing a link between membrane microdomains and the formation of polarized membrane structures involved in T cell recognition. ***The Journal of Immunology*****, 2012, 189: 689–700.**

Both immune and virological synapses involve the local accumulation of receptors on the T cell plasma membrane to enable activation or viral entry, respectively. Clustering of receptors is regulated by their compartmentalization into specialized domains or "islands" (1, 2) such as lipid rafts or tetraspanin-enriched microdomains (TEMs) or through connections to the underlying cytoskeleton (3). In addition, extensive cytoskeletal rearrangements are essential for downstream signaling events (4).

TEMs form specialized platforms on the plasma membrane that incorporate a number of adhesion-related receptors and therefore regulate their functions in terms of avidity and intracellular signaling (3). In the immune system, TEMs regulate cognate interactions both in T lymphocytes and in APCs. CD3, CD4, or CD8 associate with TEMs (3), and in APCs, TEMs include MHC molecules (5–7). Moreover, tetraspanin CD81 forms part of the BCR, and CD81-deficient mice show several defects in T-dependent B cell functions (8). We have previously reported that tetraspanin CD81 actively relocalizes to the central supramolecular activation cluster (cSMAC) during the formation of the immune synapse (9).

TEMs are also involved in viral infection, especially by human T cell leukemia virus and HIV (10–12). Both these viruses induce the formation of virological synapses, which are cell–cell contacts between infected and uninfected cells that enhance viral transmission from cell to cell. Tetraspanin CD81 specifically regulates several steps of the HIV cycle, from cell–cell fusion to viral egress (13–19).

One important molecular component of TEM is the EWI motif-containing protein 2 (EWI-2; also known as PGRL, for PG regulatory like). EWI-2 was identified and cloned by three independent laboratories as a major tetraspanin (CD9 and CD81)-associated protein (20–22). EWI-2 contains four Ig domains in its extracellular region, of which the membrane proximal domains, the transmembrane domain, and cytoplasmic palmitoylation were reported to be responsible for association with tetraspanins (21, 23). Insertion into TEMs seems to be required for normal EWI-2 expression at the plasma membrane, at least on the oocyte (24).

Overexpression of EWI-2 alters the associative balance in TEMs, so that tetraspanin–tetraspanin interactions and interactions between tetraspanins and integrins seem to be increased (25, 26). In contrast, EWI-2 overexpression reduces the association of tetraspanins with the metalloproteinase MT1-MMP (27, 28). Expression of a truncated form of EWI-2 blocks the binding of hepatitis C virus to tetraspanin CD81 (29), thus influencing viral tropism. EWI-2 may also function as a receptor itself, as its expression has been reported to be induced in mature dendritic cells (30, 31), where it can bind to HSPA8 (31).

*Servicio de Inmunología, Hospital de la Princesa, Instituto de Investigación Sanitaria Princesa, 28006 Madrid, Spain; [†]Departamento de Biología Vascular e Inflamación, Centro Nacional de Investigaciones Cardiovasculares, 28029 Madrid, Spain; [‡]Centro de Biología Molecular Severo Ochoa, Universidad Autónoma de Madrid, 28049 Madrid, Spain; [§]Unidad de Investigación, Hospital Santa Cristina, Instituto de Investigación Sanitaria Princesa, 28009 Madrid, Spain; [¶]Servicio de Inmunobiología Molecular del Hospital Universitario Gregorio Marañon, 28009 Madrid, Spain; and [‖]Department of Pathology, Harvard Medical School, Boston, MA 02115

[1]M.G.-A. and M.S.-V. contributed equally to this work.

Received for publication December 23, 2011. Accepted for publication May 2, 2012.

This work was supported by Grants PI080794 and PI11/01645 from the Instituto de Salud Carlos III (to M.Y.-M.), Ministerio de Ciencia e Innovación Grants SAF2008-02635 and SAF2011-25834, Fundación para la Investigación y la Prevención del SIDA en España Grant 36658/07 (to F.S.-M.), Grants BIO2009-07990 from the Ministerio de Educación y Ciencia, CAM BIO/0194/2006 from Comunidad de Madrid, and RECAVA RD06/0014 from the Fondo de Investigaciones Sanitarias (Ministerio de Sanidad y Consumo, Instituto Salud Carlos III) (to J.V.).

Address correspondence and reprint requests to Dr. María Yáñez-Mó, Unidad de Investigación, Hospital Santa Cristina, Instituto de Investigación Sanitaria Princesa (IIS-IP), C/Maestro Amadeo Vives 2, 28009 Madrid, Spain. E-mail address: myanez.hlpr@salud.madrid.org

The online version of this article contains supplemental material.

Abbreviations used in this article: ABD, actin binding domain; cSMAC, central supramolecular activation cluster; Env, envelope; ERM, ezrin–radixin–moesin; EWI-2, EWI motif-containing protein 2; qPCR, quantitative PCR; SEE, superantigen-E; pSMAC, peripheral supramolecular activation cluster; siRNA, small interfering RNA; TEM, tetraspanin-enriched microdomain.

www.jimmunol.org/cgi/doi/10.4049/jimmunol.1103708

Emerging evidence points to EWI-2 as a key linker between TEMs and the actin cytoskeleton via a direct association with ezrin–radixin–moesin (ERM) actin-linkers (30). In this study, we analyze the function of EWI-2 in immune and viral synapses. We report a novel biochemical interaction between EWI-2 and α-actinin. This actin cross-linking molecule controls receptor clustering at the plasma membrane of lymphoid cells (32–34). It can also bind to integrins (35, 36) and adhesion receptors such as ICAM-1 or L-selectin (37, 38). Four isoforms of human α-actinin have been identified: the muscle isoforms 2 and 3 and the non-muscle isoforms 1 and 4 (39). α-Actinin-4 has been implicated in cancer cell progression, metastasis, and immune cell migration (40, 41). We found that similar to its actin bundling capability (42), the association of α-actinin with EWI-2 depends on PIP2 binding. Our data indicate that the dynamic association of EWI-2 with α-actinin plays different roles in the formation and maintenance of immune and viral synapses.

Materials and Methods

Cells and cell cultures

T (J77, CEM T4) and B (Raji) lymphoblastoid cell lines and Jurkat T cells expressing HIV-1 envelope (Env)-HxBc2 (Jurkat HxBc2; kindly provided by the National Institutes of Health AIDS Research and Reference Reagent Program 2002–2003) were cultured in RPMI 1640 (Flow Laboratories, Irvine, U.K.) supplemented with 10% FCS (Flow Laboratories). PBMCs from healthy donors were isolated by Ficoll-Hypaque gradient centrifugation and cultured for 2 d in RPMI 1640 medium supplemented with 10% FCS in the presence of PHA (5 g/ml) or superantigen-E (SEE) (43). Then, isolated T lymphoblasts were maintained with recombinant human IL-2 (50 U/ml) for 5 d.

Abs and reagents

Anti-CD3 (T3b, 488), anti–EWI-2 (8A12), anti-ERM (90:3), and anti-CD4 (HP2/6) Abs have been described previously (9, 13, 30). Anti-CD81 I.33.22 and 5A6 mAbs were donated by Dr. R. Vilella (Hospital Clinic, Barcelona, Spain) and Dr. S. Levy (Stanford, CA), respectively. Anti–α-actinin (which recognizes all isoforms) and anti-talin Abs were purchased from Santa Cruz. Anti–p-ERK, total ERK, p-PLCγ1, and PLCγ1 Abs were from Cell Signaling (Danvers, MA). The fluorescent cell trackers CMAC and CMTMR and fluorescent phalloidins were from Invitrogen (Paisley, U.K.).

Recombinant DNA constructs

cDNAs for EWI-2 GFP and ΔCyt GFP or mRFP were obtained by PCR from a plasmid encoding human EWI-2 cDNA (30). The 5′ primer was 5′-CGAGATCTCATGGGCGCCCTCAGGC-3′, spanning a XhoI site; and 3′ primers were 5′-CGAAGCTTCCGTTTTCGAAGCCTC-3′ (for full-length EWI-2) or 5′-CGAAGCTTGCAGCAAGTGATGGTACCAAG-3′ (for truncated EWI-2), both including a HindIII site. The PCR product was first introduced into the TopoTA vector (Invitrogen) and then subcloned into pAcGFP-N1 or mRFP-N1 (Invitrogen).

The wild-type CD81-GFP construct has been described (9). Plasmids encoding α-actinin-1-GFP, α-actinin-4-GFP, and the α-actinin-4 actin binding domain (ABD) mutant were respectively provided by Carol A. Otey (School of Medicine, University of North Carolina, Chapel Hill, NC), Dr. Jonathan Jones (Northwestern University, Chicago, IL), and Maki Murata-Hori (National University of Singapore, Singapore).

Cell transfection and silencing

J77 cells (2×10^7) were washed twice with HBSS (Cambrex) and transiently transfected by electroporation with 20 μg plasmids in Optimem medium (Life Technologies, Invitrogen) at 250 V and 1200 μF (Gene Pulser II; Bio-Rad). To knock down expression of endogenous EWI-2 (30) or α-actinin-1 or α-actinin-4 (44) selectively, RNA duplexes validated in previous reports (2 μM per sample) were electroporated or nucleofected into J77 or CEM T4 cells (10^6) using the same conditions as above or the Nucleofector kit V (program T-14) (Amaxa GmbH, Cologne, Germany). Negative oligonucleotide was from Eurogentec (Serain, Belgium). Results were confirmed with two independent sequences to eliminate off-target effects.

Conjugate formation

To distinguish APCs from T lymphocytes, the cells were alternatively loaded with fluorescent trackers. APCs were loaded by incubation for 20 min at 37°C with 2 g/ml SEE. J77 T cells (10^5 cells) were mixed with Raji cells (10^5 cells) or dendritic cells (5×10^4 cells) and incubated for 30 min at 37°C, plated onto poly-L-lysine (50 μg/ml), and fixed in 4% formaldehyde. Relocalization of markers to the immune synapse was quantified using the Synapsemeasure plugin for ImageJ (45). Briefly, by using region of interest of the same area for all measurements, the signal generated by the T–APC contact area (IS), an area of APC membrane not in contact with the T cell (B), an area of T cell membrane not in contact with the APC (T), and the background (Bg) were quantified. Bg signal was subtracted from all other measurements, and then signal accumulation at the IS relative to the rest of the T cell surface was analyzed according to the formula $(IS - B)/T$.

Flow cytometry, immunofluorescence, and confocal microscopy

Flow cytometry analyses were performed as described (30) and samples were analyzed in a FACSCanto flow cytometer (Becton Dickinson).

Cognate conjugates or CEM 1.3 target HxBc2 infected pairs were stained as described (9, 13). Briefly, samples were fixed with 4% formaldehyde and permeabilized if required during 5 min with 0.5% Triton X-100. Staining was performed with species-matched secondary Abs coupled to Alexa Fluor fluorochromes (488, 547, or 647) (Invitrogen) and samples mounted with Prolong (Invitrogen). Confocal images were obtained with a Leica TCS-SP5 confocal scanning laser microscope and analyzed with Leica confocal LAS software.

IL-2 production measurement

J77 or SEE T-lymphoblasts were cocultured with SEE-loaded or unloaded Raji B cells in a 96-well plate. Supernatants were harvested after 24 or 48 h, and IL-2 content was measured using the IL-2 ELI-pair kit (Gene-probe/Diaclone) following the manufacturer's guidelines. For quantitative PCR (qPCR) of IL-2 mRNA, conjugates were harvested after 4 h of incubation at 37°C. Total mRNA was isolated with RNeasy Plus Mini Kit (Qiagen), subjected to RT-PCR with High Capacity cDNA Reverse Transcription Kit (Applied Biosystems), followed by qPCR with Power SYBR Green PCR master mix (Applied Biosystems). IL-2 mRNA was normalized to that of β-actin and HPRT1 housekeeping genes.

For intracellular IL-2 staining, primary SEE T-lymphoblasts were cocultured with SEE-loaded or Raji B cells in a 96-well plate in the presence of brefeldin A (25 μg/ml) for 12 h, stained for EWI-2, fixed and permeabilized with 0.1% saponin, and stained with allophycocyanin-conjugated anti-human IL-2 (Becton Dickinson).

Pull-down and immunoprecipitation assays

N-terminally biotinylated peptides containing an SGSG linker sequence connected to the cytoplasmic C-terminal domains of proteins of interest were purchased from Ray Biotech (Norcross, GA): EWI-2, biotin-SGSG-CCFMKRLRKR; CD81, biotin-SGSG-CCGIRNSSVY; CD9, biotin-SGSG-CCAIRRNREMV; CD151, biotin-SGSG-YRSLKLEHY; CD82, biotin-SGSG-CRHVHSEDYSKVRKY. Each peptide (30 nmol) was conjugated to 40 μl streptavidin Sepharose (Amersham Biosciences). Pull-down assays with T lymphoblast extracts were carried out as previously described (30) and analyzed by Western blot or mass spectrometry. When indicated, 50 μg/ml PIP2 (Avanti Polar Lipids, Alabaster, AL) was added for 30 min to the cell lysates before pull-down.

J77 T cells (24×10^6) were mixed for 15 min with unloaded Raji B cells (6×10^6) (time = 0) or with Raji B cells loaded with SEE for 5, 10, or 30 min at 37°C. Cells were washed once with ice-cold PBS then lysed in 1% Nonidet P-40 in PBS containing 1 mM $CaCl_2$, 1 mM $MgCl_2$, and protease and phosphatase inhibitors (Complete, PhosSTOP; Roche). Lysates were precleared for 2 h at 4°C with protein G–Sepharose (Amersham Biosciences) and then incubated for 2 h at 4°C with anti–EWI-2 mAb immobilized on protein G–Sepharose beads. After rinsing with lysis buffer, complexes were eluted in Laemmli buffer, resolved by SDS-PAGE, and immunoblotted with anti-ERM, anti–α-actinin, or anti–EWI-2 mAbs.

Mass spectrometry

Sepharose beads coming from the pull-down assays were directly resuspended in Laemmli buffer, applied onto a SDS-PAGE gel, and subjected to the one-step in-gel trypsin digestion method (46). The resulting peptides were analyzed by LC-MS/MS using a Surveyor LC system coupled to an LTQ linear ion trap mass spectrometer (Thermo-Fisher, San Jose, CA) as previously described (47, 48). The LTQ was operated in a data-dependent MS/MS mode using the 15 most intense precursors detected in a survey scan from 400 to 1600 m/z, as described (47). Proteins were identified as previously described (49) using SEQUEST algorithm (Bioworks 3.2

package; Thermo Finnigan). The raw MS/MS files were searched against the Human Swissprot database (Uniprot release 14.0, 19,929 sequence entries for human) supplemented with the sequence of porcine trypsin. SEQUEST results were validated using the probability ratio method (49), and false discovery rates were calculated by the refined method (50). Peptide and scan counting was performed assuming as positive events those with a false discovery rate ≤5%.

HIV-1 infection

HIV NL4.3 infection was assayed in CEM 3.1 cells as described (13). Briefly, HIV NL4.3 infection of CEM 3.1 cells was carried out for 5 h at 37˚C in 96-well plates. Virus was then removed by washing (PBS) infected cells. Cell-free supernatants were harvested at 24, 48, and 72 h and assayed for p24 content. For HIV attachment and entry measurements, T cells were infected with 200 ng HIV-1 NL4.3 per million cells for 2 h at 4˚C (attachment) or 37˚C (entry). Cells were extensively washed with medium and treated with pronase (0.1 mg/ml, 2 min at 4˚C, and subsequent blocking with fetal serum) to remove viral input, fixed with 1% paraformaldehyde, permeabilized with chilled methanol and 0.1% Nonidet P-40, and stained for p24 (KC57-RD1 from Beckman-Coulter) and analyzed by flow cytometry.

Results

EWI-2 colocalizes with CD81 at the cSMAC of the immune synapse and modulates IL-2 secretion

To investigate the role of EWI-2 in T cell activation upon Ag presentation, we first assessed the localization of EWI-2 by confocal microscopy in immune conjugates. We conjugated primary T lymphoblasts or J77 T cells with superantigen-loaded B cells (Fig. 1A, 1C, respectively). EWI-2 relocalized to the T–APC contact site in both cellular models compared with CD45 distribution (Fig. 1B and data not shown). Colocalization studies with markers of cSMAC (CD3 and CD81) and peripheral supramolecular activation cluster (pSMAC) (F-actin and talin) revealed that EWI-2 accumulates at the cSMAC, colocalizing with CD3 and CD81 (Fig. 1C). Vertical sections of the contact zone revealed a cluster of EWI-2 surrounded by the pSMAC marker talin (Fig. 1A and 1C, *right panels*). We next suppressed EWI-2 expression in T cells by transfection with specific small interfering RNA (siRNA) oligonucleotides (Fig. 2A) and analyzed IL-2 production in response to conjugation with superantigen-loaded Raji B cells. We found that EWI-2 depletion induced a slight but significant increase in the levels of IL-2 in both primary T lymphoblasts and J77 T cells (Fig. 2B and 2C, respectively) compared with control cells. The levels of IL-2 secretion in resting cells remained below the detection threshold of the ELISA (data not shown). When conjugated T lymphoblasts were double stained for EWI-2 and intracellular IL-2, EWI-2–depleted cells were indeed more positive for IL-2 (Fig. 2D). This increase in cytokine secretion correlated with increased mRNA of IL-2 (Fig. 2E, 2F) and with a sustained phosphorylation of PLCγ1 and ERK, predominantly at late times of activation (Fig. 2G), suggesting that EWI-2 may act as a negative regulator of T cell activation.

To address whether the effect of EWI-2 silencing was due to alterations in TEM composition (i.e., its regulatory effect on tetraspanin stoichiometry and/or organization) or to direct interactions with intracellular effectors through its cytoplasmic tail, we

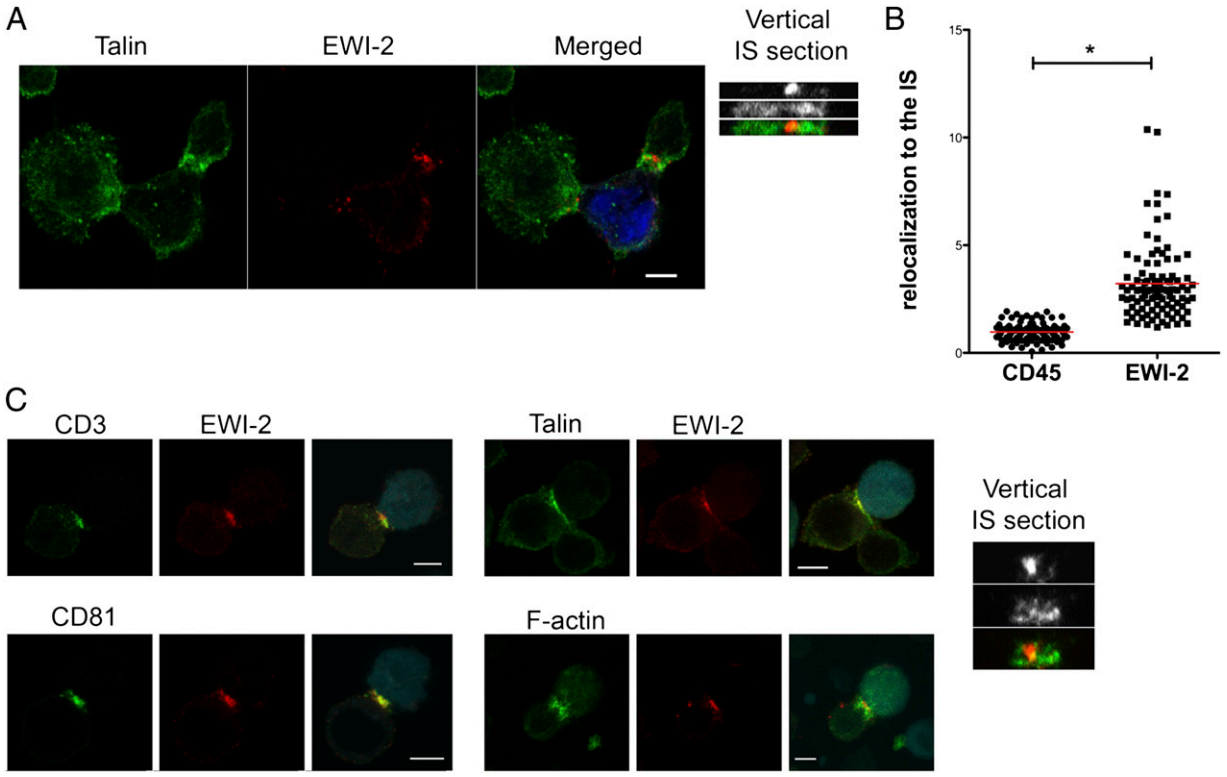

FIGURE 1. EWI-2 relocalizes to the cSMAC of the immune synapse. (**A**) Primary T lymphoblasts were conjugated with SEE-loaded CMAC-labeled (blue) Raji B cells for 30 min, fixed, and costained for EWI-2 (8A12 mAb) and talin. Maximal projections of the confocal stack are shown. *Right panel*, A vertical section of talin and EWI-2 staining in the synapse area. Scale bar, 5 μm. (**B**) Relocalization of endogenous EWI-2 and CD45 (as negative control) in conjugates formed by primary T lymphoblasts was quantified using the Synapsemeasure plugin. Data shown correspond to means ± SEM of 80 conjugates from three independent experiments. (**C**) J77 T-lymphoblastoid cells were conjugated with SEE-loaded CMAC-labeled Raji B cells (blue) for 30 min, fixed, and stained with anti-EWI-2 8A12 mAb and markers of cSMAC (anti-CD3 448 and anti-CD81 I.33.2.2) or pSMAC (F-actin and talin). Maximal projections of the confocal stacks are shown. The *right panel* in each block of three panels shows a vertical section of the synapse area in EWI-2 costaining with talin. Scale bars, 5 μm. *$p < 0.05$ (Student *t* test).

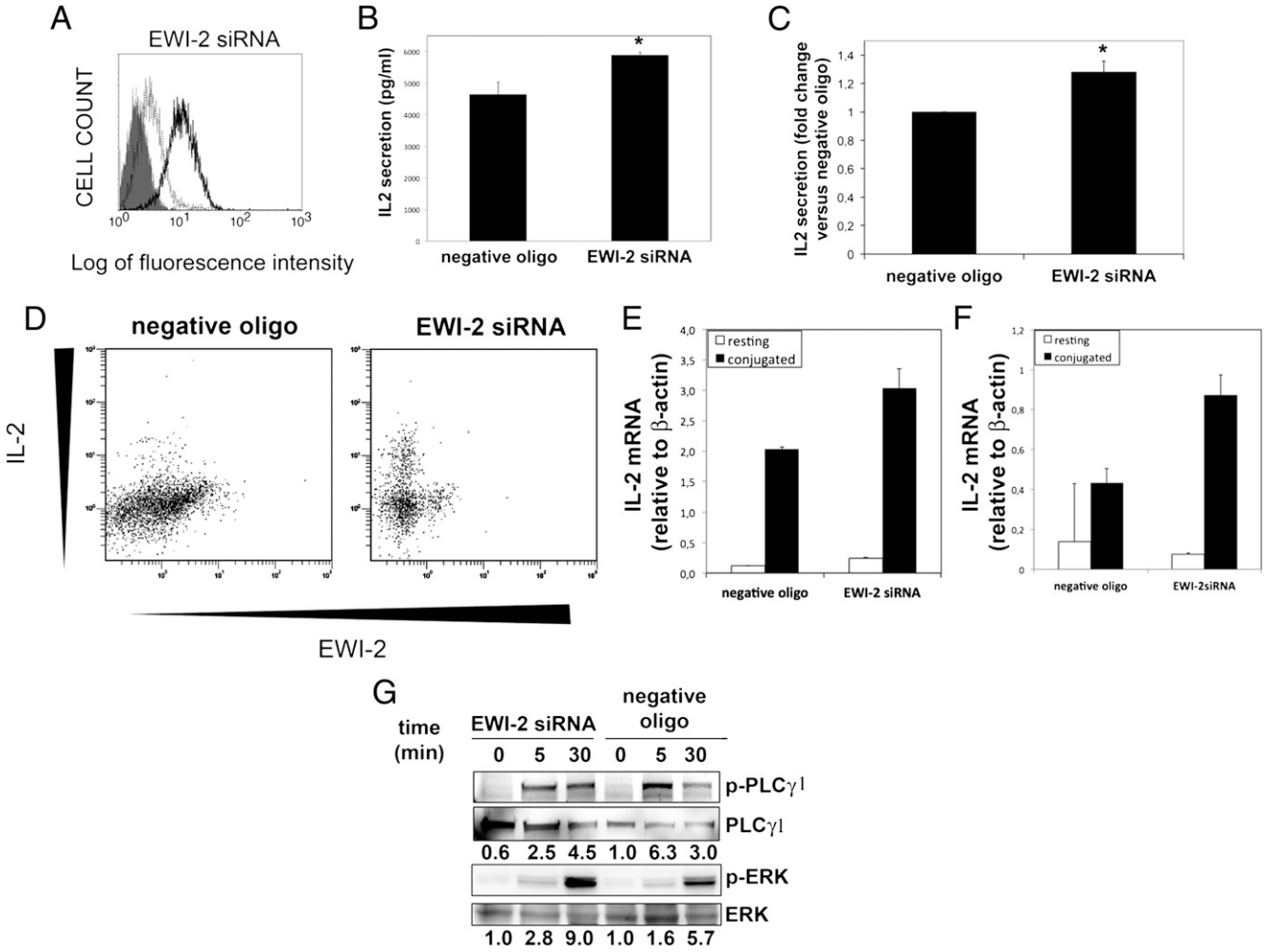

FIGURE 2. EWI-2 expression regulates T cell activation. (**A**) Flow cytometry analysis of EWI-2 silencing. Cells were stained with anti-EWI-2 8A12 mAb. Black line, J77 cells transfected with negative control oligonucleotide; gray line, cells transfected with EWI-2–specific siRNA; filled histogram, nonstained cells. (**B**) Primary T lymphoblasts were transfected with control oligonucleotide or EWI-2 siRNA. At the time of maximal knockdown, cells were conjugated overnight at a 1:1 ratio with SEE-loaded Raji B cells. Supernatants were analyzed for IL-2 content by ELISA. Data are the means ± SD of a representative experiment of three performed in triplicate. (**C**) J77 cells were transfected with control oligonucleotide or EWI-2 siRNA and treated as in (B). Data are the means ± SEM normalized to IL-2 levels in cells expressing control oligonucleotide ($n = 4$ independent experiments). (**D**) Primary T lymphoblasts were transfected with control oligonucleotide or EWI-2 siRNA. At the time of maximal knockdown, cells were conjugated overnight at a 1:1 ratio with SEE-loaded Raji B cells in the presence of brefeldin A (25 μg/ml). Cells were then double-stained for EWI-2 and intracellular IL-2. Primary T lymphoblasts (**E**) or J77 cells (**F**) were transfected with control oligonucleotide or EWI-2 siRNA. At the time of maximal knockdown, cells were conjugated for 4 h at a 1:1 ratio with SEE-loaded Raji B cells and IL-2 mRNA analyzed by qPCR. Data are the means ± SE of a representative experiment of three performed in triplicate. (**G**) J77 cells were transfected with control oligonucleotide or EWI-2 siRNA. At the time of maximal knockdown, cells were conjugated overnight at a 1:5 ratio with SEE-loaded Raji B cells for the indicated times. Total cell lysates were probed for phospho-PLCγ and phospho-ERK as well as for total PLCγ and ERK. Numbers below correspond to the quantification of phosphorylation levels of each protein, corrected for total expression of the corresponding protein and normalized to untreated control cells in a representative experiment of three performed. $*p < 0.05$ (Student t test).

compared the effects of overexpressing GFP-tagged wild-type EWI-2 and a GFP-tagged cytoplasmic deletion mutant (EWI-2-ΔCyt), which still interacts with tetraspanins and incorporates into TEM (data not shown and Ref. 26). The wild-type and ΔCyt GFP-tagged constructs were both comparably expressed on the plasma membrane of T cells (Fig. 3A, 3B). The mutant form did not relocalize to the immune synapse (Fig. 3B, 3C) and recapitulated the effects of EWI-2 silencing increasing IL-2 secretion (Fig. 3D), thereby suggesting the involvement of the EWI-2 cytoplasmic domain in T cell activation.

EWI-2 associates with α-actinin at the immune synapse in a dynamic and PIP2-dependent manner

To identify the intracellular partners of EWI-2 that regulate its localization and function during T cell activation, we performed pull-down assays on T lymphoblast lysates using biotinylated peptides corresponding to sequences from the C-terminal cytoplasmic regions of EWI-2 and tetraspanins CD81 and CD151 as baits. Mass spectrometry analysis of proteins precipitated with the EWI-2 peptide consistently detected sequences corresponding to both isoforms 1 and 4 of α-actinin (Fig. 4A and data not shown). CD81 peptides pulled down the α-actinin-1 isoform, with a lower number of peptides, but not the isoform 4 (Fig. 4B and data not shown). None of these cytoskeletal proteins were pulled down by CD151 peptides or control beads (Fig. 4B). Confirming these results, Western blot analysis of similar pull-down experiments with primary human PBLs showed that α-actinin associated predominantly with EWI-2 C-terminal peptides and more weakly with CD81 C-terminal peptides (Fig. 4C). No interactions with

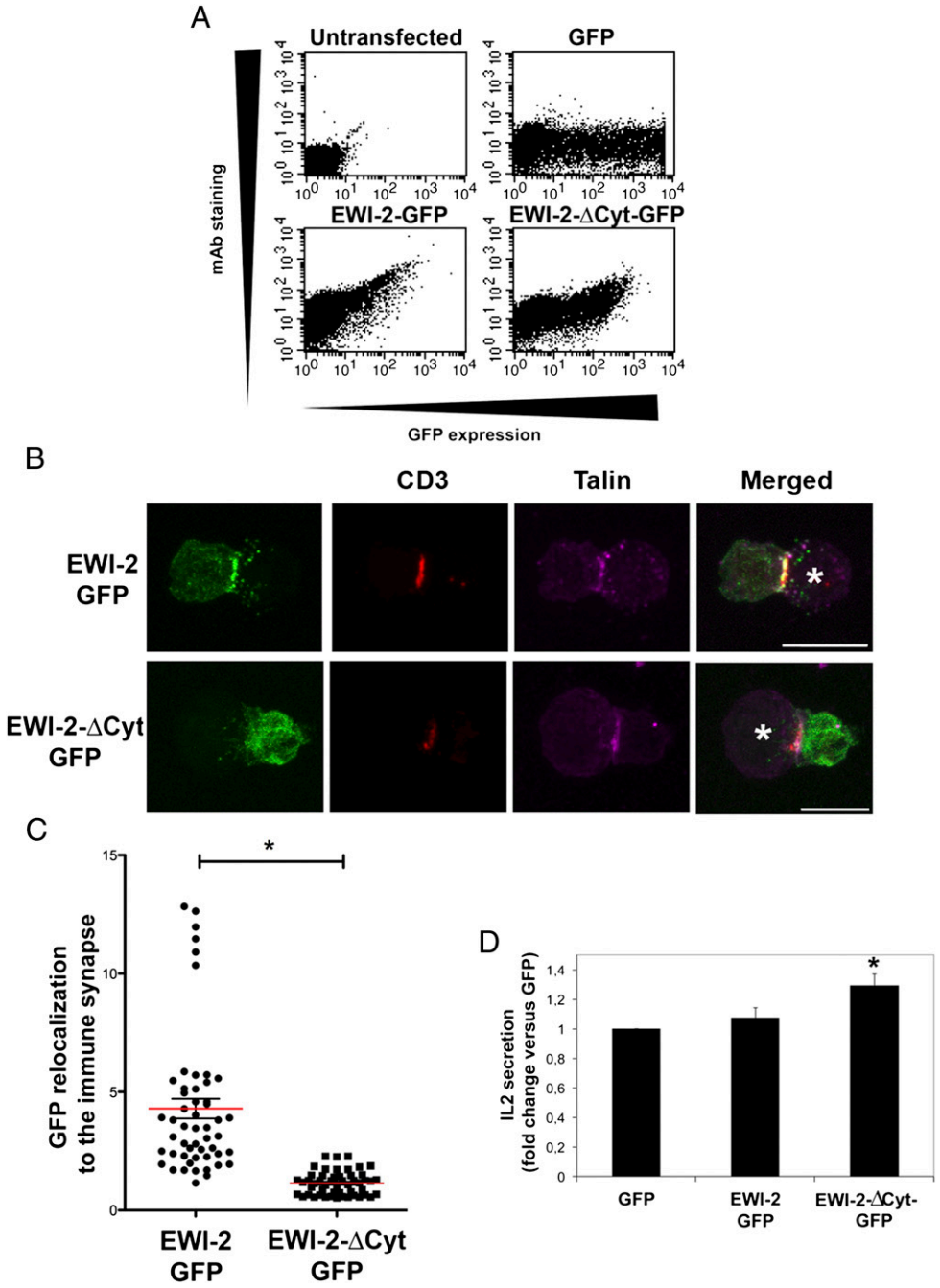

FIGURE 3. Involvement of EWI-2 cytoplasmic domain in T cell activation. (**A**) Flow cytometry analysis of the expression levels of transfected GFP-tagged wild-type EWI-2 (EWI-2-GFP) and a mutated form lacking the C-terminal cytoplasmic domain (EWI-2-ΔCyt-GFP). Cells were labeled with anti-EWI-2 8A12 mAb to check for correct expression of the tagged molecules at the plasma membrane. (**B**) Confocal immunofluorescence analysis of CD3 and talin in J77 T cells transfected with EWI-2-GFP or EWI-2-ΔCyt-GFP and conjugated with SEE-loaded Raji B cells for 30 min. Maximal projections of the confocal stack are shown. Asterisks mark Raji B cells. Scale bars, 10 μm. (**C**) GFP accumulation at the immune synapse was determined by analysis of conjugates as in (B) with the Synapsemeasure ImageJ plugin. Data are the means ± SEM of at least 20 conjugates from three independent experiments. (**D**) J77 cells were transfected with EWI-2-GFP or EWI-2-ΔCyt-GFP, conjugated overnight at a 1:1 ratio with SEE-loaded Raji B cells, and supernatants analyzed for IL-2 content by ELISA. Data are the means ± SEM normalized to IL-2 levels in cells expressing GFP alone ($n = 4$ independent experiments). *$p < 0.05$ (Student t test).

these proteins were detected for C-terminal domain peptides from tetraspanins CD9, CD151, or CD82 (Fig. 4C).

Immunostaining of endogenous α-actinin revealed its relocalization to the T–APC contact in nascent immune synapses where it colocalizes with EWI-2 at the central area. However, upon IS maturation, α-actinin moves to the peripheral zone (Fig. 5A and Supplemental Fig. 1). This kinetic behavior was further confirmed in live cell imaging (Supplemental Videos 1, 2) using fluorescently tagged EWI-2 and α-actinin, which colocalized at the cSMAC at the early stages of T–APC contact, while thereafter EWI-2 remained in the cSMAC (Fig. 5B, arrows) whereas α-actinin relocated to the pSMAC (arrowheads in Fig. 5B and Supplemental Video 2). The transient nature of EWI-2–α-actinin interaction upon IS formation was confirmed by immunoprecipitation experiments that revealed that endogenous α-actinin interacted with EWI-2 in nonstimulated T cells, although their

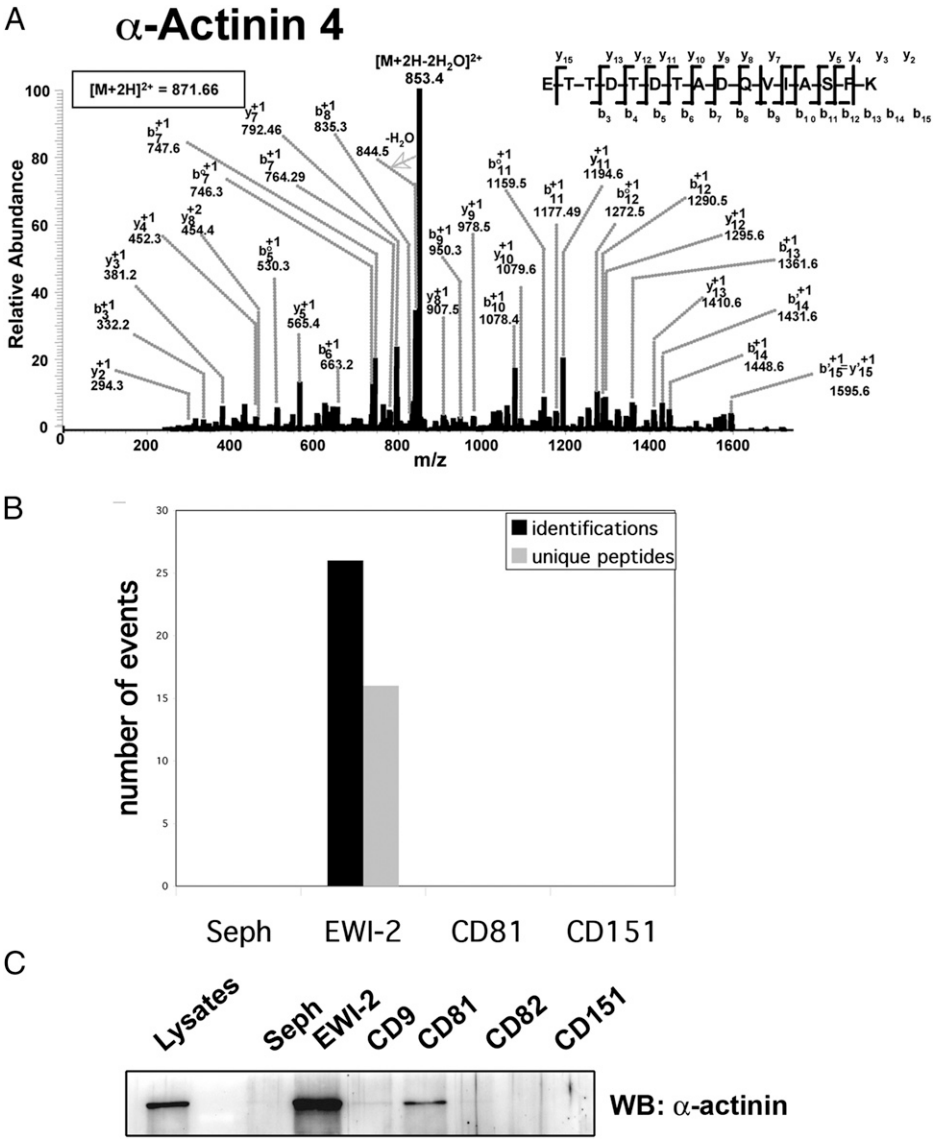

FIGURE 4. EWI-2 C-terminal domain binds to α-actinin. Proteins from primary T lymphoblast lysates precipitated with biotinylated peptides corresponding to the sequence of the EWI-2, CD81, or CD151 C-terminal cytoplasmic domains were digested and the resulting peptides identified by high-throughput mass spectrometry. (**A**) Representative MS/MS spectra of peptides belonging to α-actinin-4 in EWI-2 precipitates are shown indicating the identified peptide sequences using the nomenclature of Roepstorff and Fohlman for the main and secondary series of fragment ions. (**B**) The number of identifications and unique peptides corresponding to α-actinin-4 found in the precipitates with the different baits in a representative experiment are shown. The number of events gives an estimate of protein concentration. (**C**) Western blot analysis of the in vitro binding of α-actinin from primary T lymphoblast lysates to biotinylated peptides corresponding to the sequences of the C-terminal cytoplasmic domains of EWI-2 and tetraspanins CD81, CD9, CD82, or CD151.

association decreased rapidly upon stimulation of T cells with superantigen-loaded Raji APCs (Fig. 5C). In marked contrast, the association of other actin-binding proteins such as ERM with EWI-2 (30) did not change significantly upon superantigen stimulation (Fig. 5C).

EWI-2–α-actinin dissociation correlates with the kinetics of PIP2 accumulation during T cell activation (51). In addition, the conformation and association capability of several actin-binding proteins, including filamin, α-actinin, and ERMs, are regulated by PIP2 (52). We therefore assessed whether PIP2 regulates the association of EWI-2 with α-actinin and/or ERM proteins. We found that preincubation of T cell lysates with PIP2 reduced the association of α-actinin with the EWI-2 peptide in pull-down assays; conversely, the association with ERMs was unaffected (Fig. 5D). In contrast, PIP2 treatment induced the association of CD81 with ERM (Fig. 5D).

α-Actinin regulates actin dynamics in the immune synapse and subsequent T cell activation

To assess whether α-actinin is involved in EWI-2–dependent regulation of T cell activation, we silenced endogenous α-actinin-4 expression in T cells (Fig. 6A). Actinin silencing increased IL-2 mRNA levels, indicating that the EWI-2–actinin axis is indeed a negative regulator in T cell activation (Fig. 6B). Moreover, an additive effect was observed when both molecules were silenced (Fig. 6B). In contrast, a significant decrease in IL-2 secretion was observed in these cells upon activation with superantigen-loaded APCs, both in primary T lymphoblasts or J77 T cells (Fig. 6C, 6D), suggesting that α-actinin is also involved in downstream processes necessary to cytokine secretion. We therefore assessed the cytoskeletal architecture upon α-actinin silencing and found a reduced accumulation of F-actin and talin at the T–APC contact zone and a defective relocalization of EWI-2 to the immune synapse (Fig. 6E, 6F) resulting in a disrupted immune synapse architecture with dispersed cSMACs and pSMACs.

Overexpression of GFP-tagged wild-type α-actinin-4 also significantly reduced IL-2 secretion (Fig. 7A) correlating with an increase in the cellular F-actin content that was, however, impaired in its localization to the IS (Fig. 7B, 7C). This effect was found to rely on the actin cross-linking ability of α-actinin, as a mutant α-actinin-4 construct lacking the ABD (ActABD-GFP) did not affect IL-2 production (Fig. 7A). This mutant did not localize properly to the cellular cortex, suggesting that α-actinin may need to bind to F-actin to expose its binding site for trans-

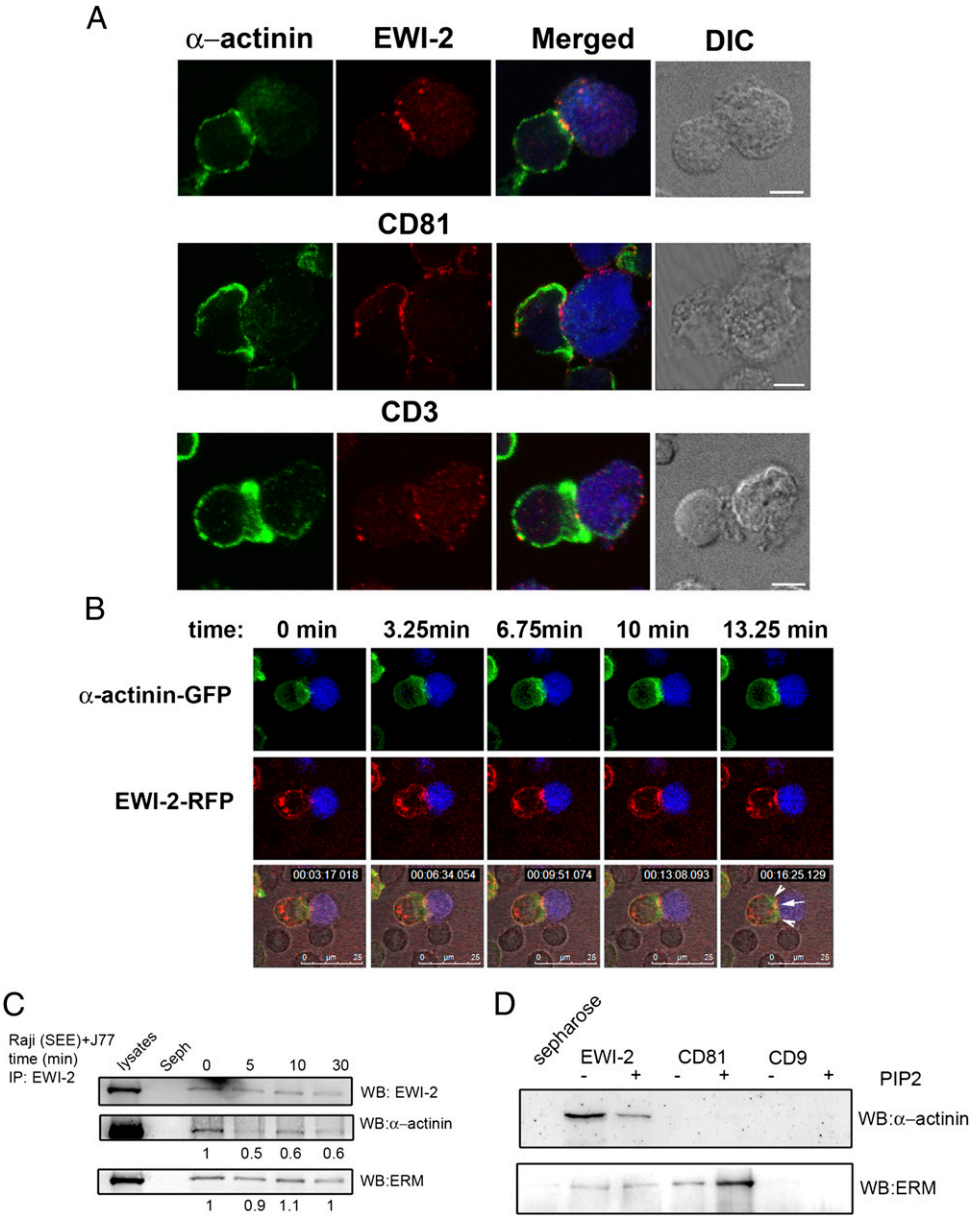

FIGURE 5. α-Actinin is a component of the immune synapse. (**A**) J77 T cells were conjugated with SEE-loaded CMAC-labeled Raji B cells (blue), fixed, permeabilized, and stained with anti–α-actinin Ab in combination with anti–EWI-2 (8A12), anti-CD81 (I.33.2.2), or anti-CD3 (T3b) mAbs. A confocal plane and the corresponding DIC image are shown. Scale bars, 5 μm. (**B**) J77 T cells were transiently transfected with GFP-tagged α-actinin-4 and RFP-tagged EWI-2 and allowed to conjugate with SEE-loaded CMAC-labeled Raji B cells (blue). Cells were monitored by time-lapse confocal microscopy at 30-s intervals. Images shown are representative maximal projections of the confocal stacks every 5 min. At later time points, α-actinin redistributes to the pSMAC (arrowheads), whereas EWI-2 remains clustered at cSMAC (arrows). Scale bars, 25 μm. (**C**) J77 T cells were conjugated 5:1 with SEE-loaded Raji B cells for the indicated times. Conjugates were then lysed and immunoprecipitated with anti-EWI-2 8A12 mAb. Blots were sequentially probed for EWI-2, α-actinin, and ERM. Numbers below the blots correspond to the quantification of the coimmunoprecipitated protein related to time 0 in a representative experiment of three performed. (**D**) Lysates from primary T lymphoblasts were incubated for 30 min with or without 50 μg/ml PIP2 and pulled down with biotinylated peptides corresponding to the C-terminal sequence of EWI-2, CD81, or CD9. Blots were sequentially probed for α-actinin and ERM. Data correspond to a representative experiment out of three.

membrane receptors such as EWI-2 (Fig. 7B). Overexpression of the ABD mutant did not affect F-actin accumulation in response to antigenic stimulation (Fig. 7C).

Thus α-actinin is involved in EWI-2–dependent T cell regulation but, in addition, affects actin dynamics and consequently the immune synapse architecture.

The EWI-2–α-actinin complex regulates HIV infection

Virological synapses share many molecular and structural features of the immunological synapse (53). In addition, TEMs modulate different phases of the HIV infective cycle (12). We and others have previously reported that knocking down CD81 either on the target or the infected cell increases syncytia formation, viral infection, and new virion infectivity, whereas it reduces viral assembly and budding (13, 17, 54, 55). Therefore, we addressed whether the EWI-2–actinin connection was functionally relevant in the membrane fusion events induced by the viral Env during HIV infection.

Both EWI-2 and α-actinin were evenly distributed on the plasma membrane of T cells and accumulated at intercellular

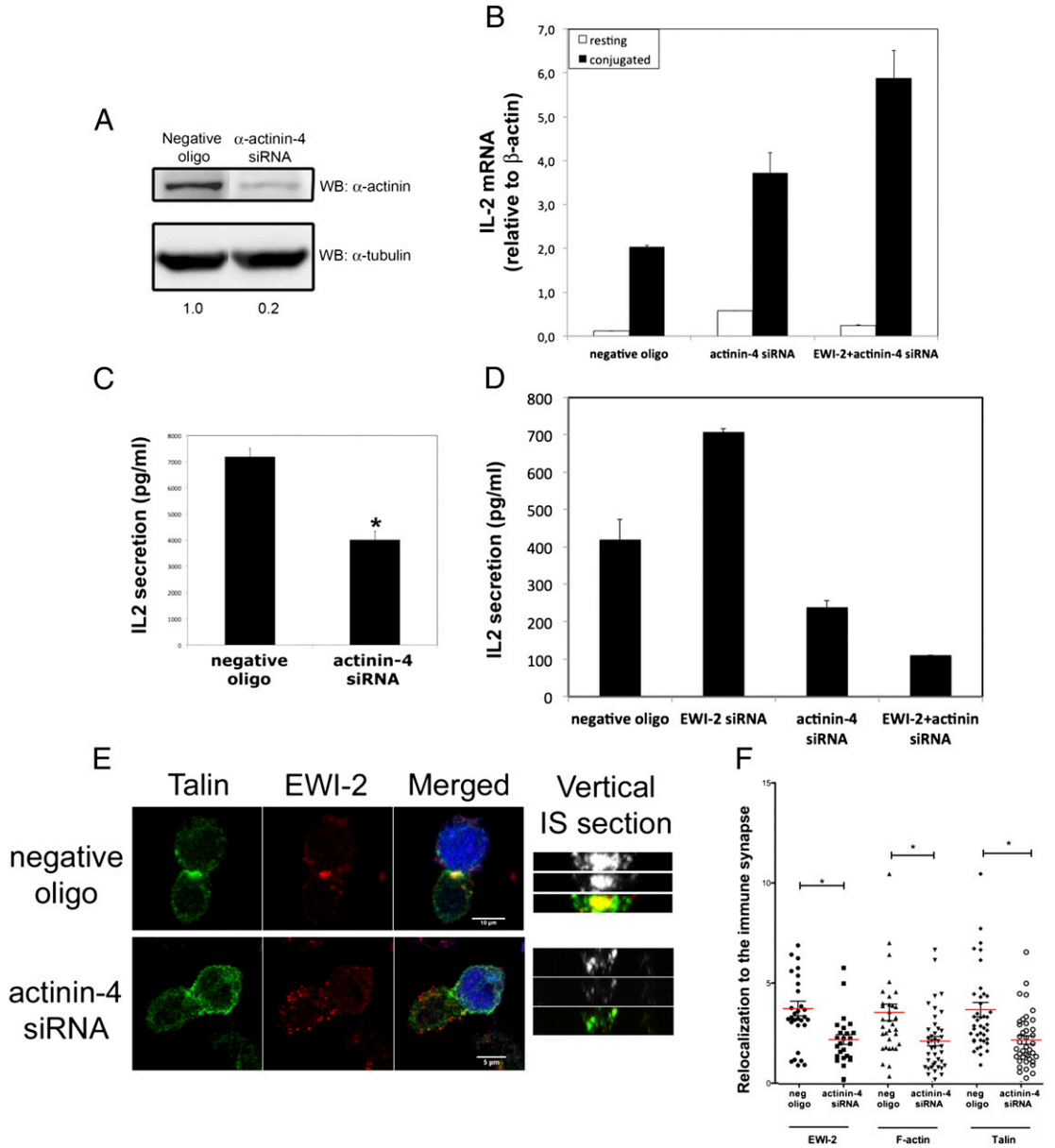

FIGURE 6. α-Actinin knockdown impairs T cell activation upon Ag presentation. (**A**) J77 cells were transfected with either negative control oligonucleotide or siRNA duplexes directed to α-actinin isoform 4. α-Actinin expression analyzed by Western blot; tubulin is shown as a loading control. Numbers indicate the relative α-actinin expression in the experiment shown, corrected for the tubulin signal and normalized to control cells. (**B**) Primary T lymphoblasts were transfected with control oligonucleotide, α-actinin-4 siRNA, or both EWI-2 and α-actinin-4 siRNA. At the time of maximal knockdown, cells were conjugated for 4 h at a 1:1 ratio with SEE-loaded Raji B cells and IL-2 mRNA analyzed by qPCR. Data are the means ± SE of a representative experiment of three performed in triplicate. (**C**) Primary T lymphoblasts were transfected with either control oligonucleotide or α-actinin isoform 4 siRNA. At the time of maximal knockdown, cells were conjugated overnight at a 1:1 ratio with SEE-loaded Raji B cells, and supernatants were analyzed for IL-2 content by ELISA. Data are the means ± SD of a representative experiment by triplicate. (**D**) J77 cells were transfected with either control oligonucleotide or EWI-2, α-actinin isoform 4 siRNA, or both, and treated as in (C). Data are the means ± SD of a representative experiment performed in triplicate. (**E**) J77 cells were transfected either with control oligonucleotide or α-actinin isoform 4 siRNA. At the time of maximal knockdown, cells were conjugated with SEE-loaded CMAC-labeled (blue) Raji B cells for 30 min, fixed, and stained for EWI-2 and talin. Maximal projections of the confocal stacks are shown together with a vertical section of the immune synapse area. Scale bars, 5 μm. (**F**) Analysis of conjugates stained as in (C) with the Synapsemeasure ImageJ plugin. Data are the means ± SEM of at least 20 conjugates from three independent experiments. *$p < 0.05$ (Student t test).

contacts between uninfected cells and cells expressing HIV-1 Env proteins (Fig. 8A). We found increased virus production and syncytia formation in EWI-2–silenced T cells postinfection with HIV-1 NL4.3 viral particles (Fig. 8B and data not shown). Overexpression of wild-type EWI-2 did not significantly affect HIV infection, whereas overexpression of EWI-2-ΔCyt mimicked the effect of EWI-2 silencing, increasing viral production (Fig. 8B).

Notably, higher titers of new HIV virions were also produced in target T cells silenced for α-actinin-4 (Fig. 8C). Overexpression of the α-actinin-4 mutant Act-ABD-GFP also enhanced the viral titers (Fig. 8C), whereas overexpression of GFP-tagged α-actinin-4 had no significant effect (Fig. 8C) suggesting that the actin cross-linking activity of α-actinin is essential for its limiting effect on HIV infection. To explore, which phase of the viral cycle was being affected by α-actinin, we measured viral attachment (incubating the target cells for 2 h with the virions at 4°C) or the subsequent entry step (with a 2-h incubation at 37°C). Actinin depletion did not affect the attachment of HIV virions to the cell

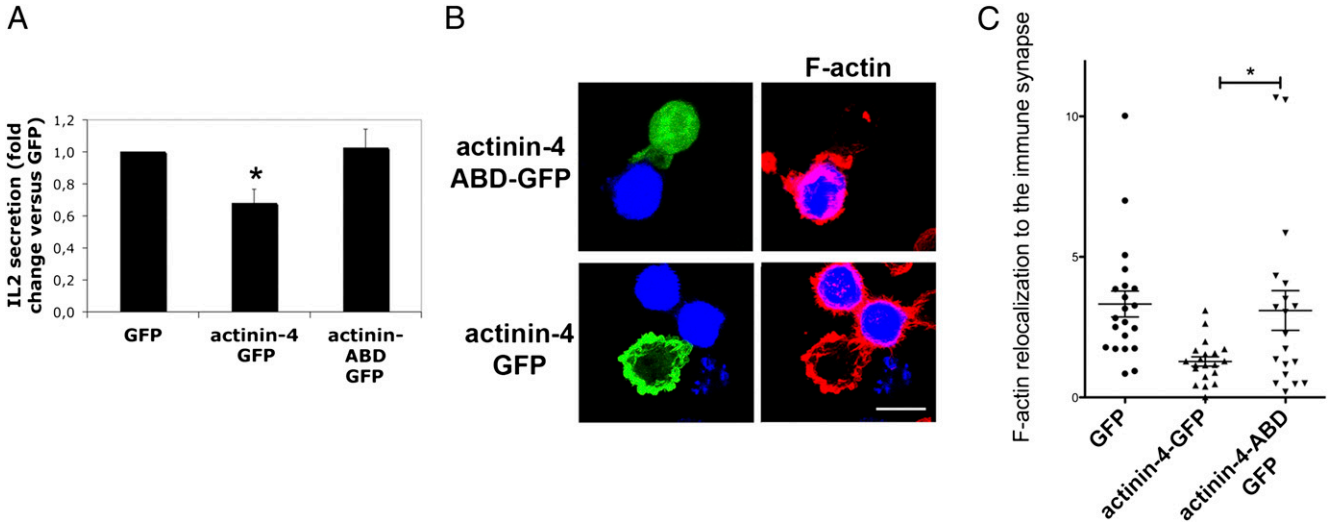

FIGURE 7. α-Actinin overexpression impairs F-actin relocalization to the immune synapse. (**A**) J77 cells were transfected with GFP-tagged wild-type α-actinin-4 or a GFP-tagged truncated mutant lacking the ABD and conjugated overnight at a 1:1 ratio with SEE-loaded Raji B cells. Supernatants were analyzed for IL-2 content by ELISA. Data are the means ± SEM normalized to IL-2 levels in cells expressing GFP alone ($n = 3$ independent experiments). (**B**) Cells transfected as in (A) were conjugated for 30 min with SEE-loaded CMAC-labeled Raji B cells (blue), stained for F-actin, and analyzed by confocal microscopy. Images are maximal projections of the confocal stacks. Scale bar, 10 μm. (**C**) Analysis of conjugates stained as in (B) with the Synapsemeasure ImageJ plugin. Data are the means ± SEM of at least 20 conjugates from three independent experiments. *$p < 0.05$ (Student t test).

surface but enhanced their entry into the cell, further reinforcing its functional role in actin remodeling during HIV infection (Fig. 8D).

Discussion

The formation of the immune synapse in T cells proceeds through a series of rearrangement of membrane receptors at the plasma membrane. Ag presentation has to reach tremendous sensitivity with fast dynamics so that a TCR appropriately signals after encounter with a single peptide–MHC complex during scanning on an APC surface (56, 57). For that purpose, signaling and adhesion receptors occur in preassembled protein islands or microdomains at the plasma membrane (1, 2). In the formation of these preassembled signalosomes, protein–protein as well as protein–lipid interactions play an important role (2, 58). Tetraspanin-enriched microdomains are good candidates to encompass all these functional characteristics for the TCR microdomains. Indeed, tetraspanins associate with both CD4 and CD8 coreceptors and weakly with CD3 (59). Moreover, tetraspanins are relocalized to the cSMAC during Ag-induced immune synapse formation (9).

EWI-2 is directly and strongly associated with tetraspanins CD81 and CD9 (21, 22). Although it may also function as a receptor itself (31), in most instances is seems to regulate the internal stoichiometry of tetraspanin-enriched microdomains (25, 26, 28), conceivably by competing with other lower-affinity partners. Our data suggest that in the immune synapse, the main function for EWI-2 appears to be the connection of TEMs with the underlying cytoskeleton. Hence, overexpression of wild-type EWI-2 did not alter the immune synapse architecture or IL-2 secretion levels. However, a mutant EWI-2 devoid of its cytoplasmic domain, which can insert into tetraspanin-enriched microdomains (26) but is unable to link them properly to the actin cytoskeleton, had a dominant negative effect and recapitulated the phenotype of EWI-2–silenced cells.

EWI-2 cytoplasmic domain can bind to ERM proteins (30) and α-actinin. Two isoforms of α-actinin, 1 and 4, are expressed in T cells. Although we have focused our study on α-actinin-4 due to its apparent higher binding to EWI-2, silencing of α-actinin-1 induced similar changes in T cell activation and HIV infection (data not shown), suggesting that the key role of α-actinin in the formation of IS and viral synapse formation relies on its actin cross-linking activity. All these cytoskeletal components play a functional role in the organization of the immune synapse architecture as demonstrated in this study and in previous reports (60, 61). A high degree of redundancy is often observed in the associations of TEMs with the actin cytoskeleton (3). Indeed, tetraspanin CD81 is also able to bind to ERMs and α-actinin-1, but its lower affinity may not be sufficient by itself to maintain the TEM association to the cortical meshwork in an in vivo situation.

Our data indicate that the association of EWI-2 with different actin-linker proteins is dynamically regulated during the immune synapse formation. Thus, right after early activation, EWI-2 dissociates from α-actinin in a PIP2-dependent manner. This dissociation correlates with the segregation of the cSMAC, which is pretty much devoid of actin (62), and the pSMAC, where the cell–cell adhesion molecules and the actin meshwork concentrate. PIP2-induced dissociation of EWI-2 from actinin may be an important step in the arrangement of the architecture of the immune synapse. Thus, EWI-2 silencing or overexpression of the cytoplasmic deletion mutant might facilitate the disconnection from the actin meshwork of the signaling components of the immune synapse that gather at the cSMAC, explaining the opposite final outcome on T cell activation and IL-2 secretion attained after EWI-2 or actinin silencing.

Actin dynamics is important at different levels of the Ag presentation process. First, it participates in the organization of the membrane microdomains and the signaling complexes that initiate the signaling cascade (1, 2). In a second phase, actin flow redistributes these complexes so that supramolecular activation clusters are segregated on the cell–cell contact surface (63), and actin peripheral bundles sustain intercellular adhesion. Third, the actin meshwork serves as scaffold for the coordination of signaling cascades downstream of the TCR and costimulatory molecules (4, 57, 64). Finally, it coordinates with the tubulin cytoskeleton (61, 65) and the intracellular vesicular compartment (45) that translocates to the immune synapse providing molecular components necessary for the second wave of late signaling (65). Our data indicate that downstream of tetraspanin-enriched microdomains,

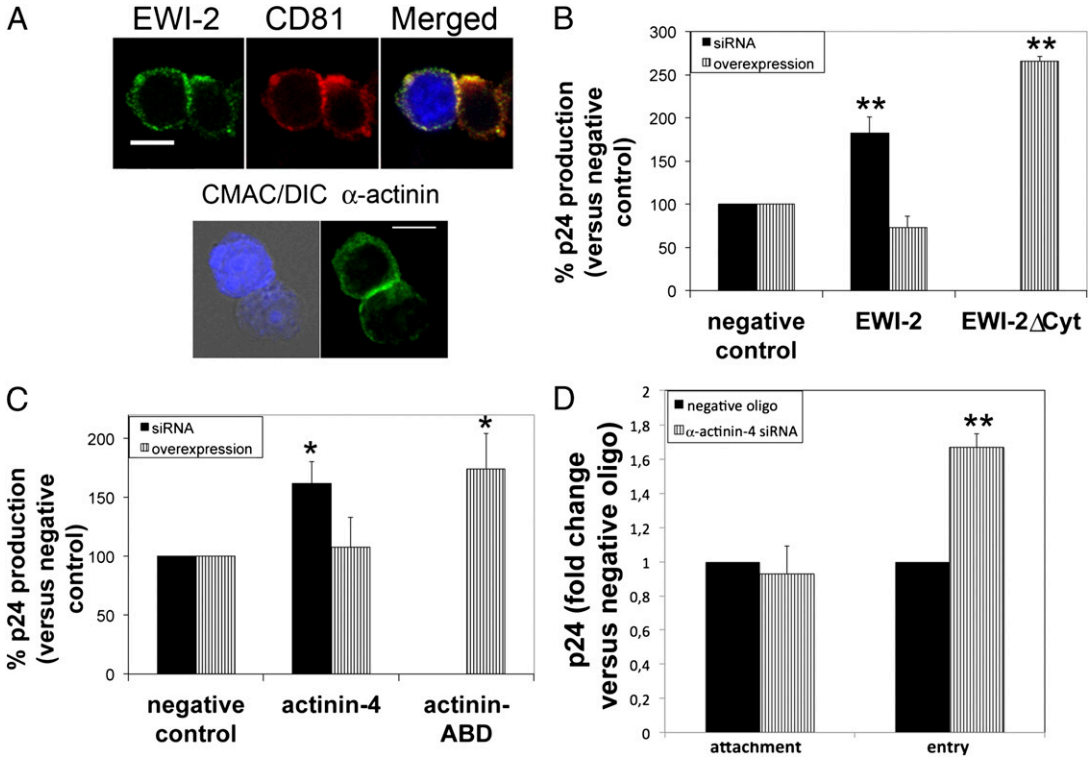

FIGURE 8. Levels of EWI-2 and α-actinin expression regulate HIV infection. (**A**) Target CEM 1.3 cells were incubated for 3 h with CMAC-labeled Env HxBc2 cells (blue), and cells were fixed and costained for EWI-2 and CD81 or for α-actinin. Scale bars, 5 and 10 μm, respectively. (**B**) Target CEM 1.3 cells were transfected with negative control oligonucleotide or EWI-2 siRNA (black bars) or with GFP (negative control), GFP-tagged wild-type EWI-2, or GFP-tagged EWI-2-ΔCyt (lacking the C-terminal cytoplasmic domain). At the time of maximal expression or knockdown, cells were infected with fully competent HIV-1 NL4-3. Cell-free supernatants were harvested at 72 h postinfection. Virus production was measured by p24-ELISA and is represented as the mean ± SEM relative to negative controls. Data are from a minimum of five independent experiments performed in triplicate. (**C**) Target CEM 1.3 cells were transfected with negative control oligonucleotide or α-actinin-4 siRNA (black bars) or with GFP (negative control), GFP-tagged wild-type α-actinin-4, or GFP-tagged α-actinin-ABD (truncated mutant lacking the ABD). At the time of maximal expression or knockdown, cells were infected with fully competent HIV-1 NL4-3. Cell-free supernatants were harvested at 72 h postinfection. Virus production was measured by p24-ELISA and is represented as the mean ± SD relative to negative controls. Data are from a minimum of two independent experiments performed in triplicate. (**D**) Effect of α-actinin-4 silencing on HIV-1 attachment (4°C) and entry (37°C) into target T cells. Data present the fold change relative to control in the percentage of positive cells for intracellular p24 by flow cytometry (mean ± SD of triplicates). $*p < 0.05$, $**p < 0.01$ (Student t test).

α-actinin regulates the actin rearrangements that take place during the immune synapse formation. α-Actinin silencing has the same enhancing effect on IL-2 transcription as that of EWI-2 silencing but, in addition, impairs cytoskeletal rearrangements, leading to a diminished cytokine secretion. In accordance, overexpression induces an increment on F-actin content that is, however, not properly relocalized to the IS, and as a consequence cytokine secretion is also reduced, reinforcing the notion that adequate actin dynamics and correct polarization are fundamental for proper T cell activation (4, 57, 64). Silencing of both EWI-2 and actinin resulted in an additive effect in IL-2 mRNA transcription and in a more pronounced inhibition of cytokine secretion. However, this effect could be related to the fact that double silencing resulted in an increased diminution of the expression of both molecules compared with silencing of them separately (data not shown).

HIV hijacks several components of the T cell activation machinery during its infectious cycle. In that regard, our data indicate that TEMs are also involved in the early steps of membrane fusion events (Ref. 13 and this study) and that TEM connections with the underlying cytoskeleton are also modulated by the virions. It is interesting to note, however, that despite the molecular and dynamic similarities between immune and viral synapses, the functional outcome of the regulation of actin dynamics by α-actinin fundamentally differs in these two types of contacts. During HIV infection, α-actinin hampers viral infection, and this effect is related to its actin cross-linking activity, as demonstrated by the effect of a mutant unable to bind to F-actin. This is consistent with the proposed role of polymerized and cross-linked actin as a physical barrier that opposes HIV-1 entry (66–68). Again, this process is dynamically governed by PIP2. During the early steps of HIV infection, a PIP2 burst occurs (69), which would lower α-actinin affinity for actin (42) and EWI-2 (this study). In this manner, a local increase of PIP2 caused by viral attachment would release α-actinin and locally inhibit its actin bundling activity (70) allowing the "softening" and rearrangement of the cortical actin cytoskeleton to proceed to viral entry. Such rearrangements are mediated, at least in part, by other actin-binding proteins such as moesin (71) so that, in this scenario, α-actinin and moesin play opposite roles. Although our data point to the role of actinin in HIV entry, we cannot exclude the involvement of the EWI-2–actinin axis in subsequent steps of the viral cycle.

In summary, our results show that EWI-2–α-actinin complexes are functionally important regulators of T cell activation and HIV-1 infection. However, the actin cross-linking capacity of α-actinin promotes different outcomes, being required for a correct configuration of the architecture of the immune synapse during Ag presentation but inhibiting the entry of the virus into the cell.

Acknowledgments

We thank S. Bartlett for English editing, Dr. Vicente-Manzanares for critical reading of the manuscript, and F. Baixauli for assistance with qPCR.

Disclosures

The authors have no financial conflicts of interest.

References

1. Lillemeier, B. F., M. A. Mörtelmaier, M. B. Forstner, J. B. Huppa, J. T. Groves, and M. M. Davis. 2010. TCR and Lat are expressed on separate protein islands on T cell membranes and concatenate during activation. *Nat. Immunol.* 11: 90–96.
2. Sherman, E., V. Barr, S. Manley, G. Patterson, L. Balagopalan, I. Akpan, C. K. Regan, R. K. Merrill, C. L. Sommers, J. Lippincott-Schwartz, and L. E. Samelson. 2011. Functional nanoscale organization of signaling molecules downstream of the T cell antigen receptor. *Immunity* 35: 705–720.
3. Yáñez-Mó, M., O. Barreiro, M. Gordon-Alonso, M. Sala-Valdés, and F. Sánchez-Madrid. 2009. Tetraspanin-enriched microdomains: a functional unit in cell plasma membranes. *Trends Cell Biol.* 19: 434–446.
4. Gordón-Alonso, M., E. Veiga, and F. Sánchez-Madrid. 2010. Actin dynamics at the immunological synapse. *Cell Health Cytoskel.* 2: 33–47.
5. Unternaehrer, J. J., A. Chow, M. Pypaert, K. Inaba, and I. Mellman. 2007. The tetraspanin CD9 mediates lateral association of MHC class II molecules on the dendritic cell surface. *Proc. Natl. Acad. Sci. USA* 104: 234–239.
6. Engering, A., and J. Pieters. 2001. Association of distinct tetraspanins with MHC class II molecules at different subcellular locations in human immature dendritic cells. *Int. Immunol.* 13: 127–134.
7. Lagaudrière-Gesbert, C., S. Lebel-Binay, E. Wiertz, H. L. Ploegh, D. Fradelizi, and H. Conjeaud. 1997. The tetraspanin protein CD82 associates with both free HLA class I heavy chain and heterodimeric beta 2-microglobulin complexes. *J. Immunol.* 158: 2790–2797.
8. Levy, S., S. C. Todd, and H. T. Maecker. 1998. CD81 (TAPA-1): a molecule involved in signal transduction and cell adhesion in the immune system. *Annu. Rev. Immunol.* 16: 89–109.
9. Mittelbrunn, M., M. Yáñez-Mó, D. Sancho, A. Ursa, and F. Sánchez-Madrid. 2002. Cutting edge: dynamic redistribution of tetraspanin CD81 at the central zone of the immune synapse in both T lymphocytes and APC. *J. Immunol.* 169: 6691–6695.
10. Hassuna, N., P. N. Monk, G. W. Moseley, and L. J. Partridge. 2009. Strategies for targeting tetraspanin proteins: potential therapeutic applications in microbial infections. *BioDrugs* 23: 341–359.
11. Ono, A. 2010. Relationships between plasma membrane microdomains and HIV-1 assembly. *Biol. Cell* 102: 335–350.
12. van Spriel, A. B., and C. G. Figdor. 2010. The role of tetraspanins in the pathogenesis of infectious diseases. *Microbes Infect.* 12: 106–112.
13. Gordón-Alonso, M., M. Yañez-Mó, O. Barreiro, S. Alvarez, M. A. Muñoz-Fernández, A. Valenzuela-Fernández, and F. Sánchez-Madrid. 2006. Tetraspanins CD9 and CD81 modulate HIV-1-induced membrane fusion. *J. Immunol.* 177: 5129–5137.
14. Garcia, E., M. Pion, A. Pelchen-Matthews, L. Collinson, J. F. Arrighi, G. Blot, F. Leuba, J. M. Escola, N. Demaurex, M. Marsh, and V. Piguet. 2005. HIV-1 trafficking to the dendritic cell-T-cell infectious synapse uses a pathway of tetraspanin sorting to the immunological synapse. *Traffic* 6: 488–501.
15. Grigorov, B., V. Attuil-Audenis, F. Perugi, M. Nedelec, S. Watson, C. Pique, J. L. Darlix, H. Conjeaud, and D. Muriaux. 2009. A role for CD81 on the late steps of HIV-1 replication in a chronically infected T cell line. *Retrovirology* 6: 28.
16. Jolly, C., and Q. J. Sattentau. 2007. Human immunodeficiency virus type 1 assembly, budding, and cell-cell spread in T cells take place in tetraspanin-enriched plasma membrane domains. *J. Virol.* 81: 7873–7884.
17. Sato, K., J. Aoki, N. Misawa, E. Daikoku, K. Sano, Y. Tanaka, and Y. Koyanagi. 2008. Modulation of human immunodeficiency virus type 1 infectivity through incorporation of tetraspanin proteins. *J. Virol.* 82: 1021–1033.
18. Deneka, M., A. Pelchen-Matthews, R. Byland, E. Ruiz-Mateos, and M. Marsh. 2007. In macrophages, HIV-1 assembles into an intracellular plasma membrane domain containing the tetraspanins CD81, CD9, and CD53. *J. Cell Biol.* 177: 329–341.
19. Nydegger, S., S. Khurana, D. N. Krementsov, M. Foti, and M. Thali. 2006. Mapping of tetraspanin-enriched microdomains that can function as gateways for HIV-1. *J. Cell Biol.* 173: 795–807.
20. Charrin, S., F. Le Naour, V. Labas, M. Billard, J. P. Le Caer, J. F. Emile, M. A. Petit, C. Boucheix, and E. Rubinstein. 2003. EWI-2 is a new component of the tetraspanin web in hepatocytes and lymphoid cells. *Biochem. J.* 373: 409–421.
21. Clark, K. L., Z. Zeng, A. L. Langford, S. M. Bowen, and S. C. Todd. 2001. PGRL is a major CD81-associated protein on lymphocytes and distinguishes a new family of cell surface proteins. *J. Immunol.* 167: 5115–5121.
22. Stipp, C. S., T. V. Kolesnikova, and M. E. Hemler. 2001. EWI-2 is a major CD9 and CD81 partner and member of a novel Ig protein subfamily. *J. Biol. Chem.* 276: 40545–40554.
23. Montpellier, C., B. A. Tews, J. Poitrimole, V. Rocha-Perugini, V. D'Arienzo, J. Potel, X. A. Zhang, E. Rubinstein, J. Dubuisson, and L. Cocquerel. 2011. Interacting regions of CD81 and two of its partners, EWI-2 and EWI-2wint, and their effect on hepatitis C virus infection. *J. Biol. Chem.* 286: 13954–13965.
24. He, Z. Y., S. Gupta, D. Myles, and P. Primakoff. 2009. Loss of surface EWI-2 on CD9 null oocytes. *Mol. Reprod. Dev.* 76: 629–636.
25. Kolesnikova, T. V., C. S. Stipp, R. M. Rao, W. S. Lane, F. W. Luscinskas, and M. E. Hemler. 2004. EWI-2 modulates lymphocyte integrin alpha4beta1 functions. *Blood* 103: 3013–3019.
26. Stipp, C. S., T. V. Kolesnikova, and M. E. Hemler. 2003. EWI-2 regulates alpha3beta1 integrin-dependent cell functions on laminin-5. *J. Cell Biol.* 163: 1167–1177.
27. Yañez-Mó, M., O. Barreiro, P. Gonzalo, A. Batista, D. Megías, L. Genís, N. Sachs, M. Sala-Valdés, M. A. Alonso, M. C. Montoya, et al. 2008. MT1-MMP collagenolytic activity is regulated through association with tetraspanin CD151 in primary endothelial cells. *Blood* 112: 3217–3226.
28. Kolesnikova, T. V., A. R. Kazarov, M. E. Lemieux, M. A. Lafleur, S. Kesari, A. L. Kung, and M. E. Hemler. 2009. Glioblastoma inhibition by cell surface immunoglobulin protein EWI-2, in vitro and in vivo. *Neoplasia* 11: 77–86, 4p, 86.
29. Rocha-Perugini, V., C. Montpellier, D. Delgrange, C. Wychowski, F. Helle, A. Pillez, H. Drobecq, F. Le Naour, S. Charrin, S. Levy, E. Rubinstein, J. Dubuisson, and L. Cocquerel. 2008. The CD81 partner EWI-2wint inhibits hepatitis C virus entry. *PLoS One* 3: e1866.
30. Sala-Valdés, M., A. Ursa, S. Charrin, E. Rubinstein, M. E. Hemler, F. Sánchez-Madrid, and M. Yáñez-Mó. 2006. EWI-2 and EWI-F link the tetraspanin web to the actin cytoskeleton through their direct association with ezrin-radixin-moesin proteins. *J. Biol. Chem.* 281: 19665–19675.
31. Kettner, S., F. Kalthoff, P. Graf, E. Priller, F. Kricek, I. Lindley, and T. Schweighoffer. 2007. EWI-2/CD316 is an inducible receptor of HSPA8 on human dendritic cells. *Mol. Cell. Biol.* 27: 7718–7726.
32. Kellie, S., B. Patel, E. J. Pierce, and D. R. Critchley. 1983. Capping of cholera toxin-ganglioside GM1 complexes on mouse lymphocytes is accompanied by co-capping of alpha-actinin. *J. Cell Biol.* 97: 447–454.
33. Geiger, B., and S. J. Singer. 1979. The participation of alpha-actinin in the capping of cell membrane components. *Cell* 16: 213–222.
34. Hoessli, D., E. Rungger-Brändle, B. M. Jockusch, and G. Gabbiani. 1980. Lymphocyte alpha-actinin. Relationship to cell membrane and co-capping with surface receptors. *J. Cell Biol.* 84: 305–314.
35. Stanley, P., A. Smith, A. McDowall, A. Nicol, D. Zicha, and N. Hogg. 2008. Intermediate-affinity LFA-1 binds alpha-actinin-1 to control migration at the leading edge of the T cell. *EMBO J.* 27: 62–75.
36. Otey, C. A., F. M. Pavalko, and K. Burridge. 1990. An interaction between alpha-actinin and the beta 1 integrin subunit in vitro. *J. Cell Biol.* 111: 721–729.
37. Carpén, O., P. Pallai, D. E. Staunton, and T. A. Springer. 1992. Association of intercellular adhesion molecule-1 (ICAM-1) with actin-containing cytoskeleton and alpha-actinin. *J. Cell Biol.* 118: 1223–1234.
38. Pavalko, F. M., D. M. Walker, L. Graham, M. Goheen, C. M. Doerschuk, and G. S. Kansas. 1995. The cytoplasmic domain of L-selectin interacts with cytoskeletal proteins via alpha-actinin: receptor positioning in microvilli does not require interaction with alpha-actinin. *J. Cell Biol.* 129: 1155–1164.
39. Oikonomou, K. G., K. Zachou, and G. N. Dalekos. 2011. Alpha-actinin: a multidisciplinary protein with important role in B-cell driven autoimmunity. *Autoimmun. Rev.* 10: 389–396.
40. Menez, J., B. Le Maux Chansac, G. Dorothée, I. Vergnon, A. Jalil, M. F. Carlier, S. Chouaib, and F. Mami-Chouaib. 2004. Mutant alpha-actinin-4 promotes tumorigenicity and regulates cell motility of a human lung carcinoma. *Oncogene* 23: 2630–2639.
41. Niggli, V., and V. Jenni. 1989. Actin-associated proteins in human neutrophils: identification and reorganization upon cell activation. *Eur. J. Cell Biol.* 49: 366–372.
42. Fraley, T. S., T. C. Tran, A. M. Corgan, C. A. Nash, J. Hao, D. R. Critchley, and J. A. Greenwood. 2003. Phosphoinositide binding inhibits alpha-actinin bundling activity. *J. Biol. Chem.* 278: 24039–24045.
43. Robles-Valero, J., N. B. Martín-Cófreces, A. Lamana, S. Macdonald, Y. Volkov, and F. Sánchez-Madrid. 2010. Integrin and CD3/TCR activation are regulated by the scaffold protein AKAP450. *Blood* 115: 4174–4184.
44. Celli, L., J. J. Ryckewaert, E. Delachanal, and A. Duperray. 2006. Evidence of a functional role for interaction between ICAM-1 and nonmuscle alpha-actinins in leukocyte diapedesis. *J. Immunol.* 177: 4113–4121.
45. Calabia-Linares, C., J. Robles-Valero, H. de la Fuente, M. Perez-Martinez, N. Martín-Cofreces, M. Alfonso-Pérez, C. Gutierrez-Vázquez, M. Mittelbrunn, S. Ibiza, F. R. Urbano-Olmos, et al. 2011. Endosomal clathrin drives actin accumulation at the immunological synapse. *J. Cell Sci.* 124: 820–830.
46. Bonzon-Kulichenko, E., D. Perez-Hernandez, E. Nunez, P. Martinez-Acedo, P. Navarro, M. Trevisan-Herraz, C. Ramos Mdel, S. Sierra, S. Martinez-Martinez, M. Ruiz-Meana, et al. 2011. A robust method for quantitative high-throughput analysis of proteomes by 18O labeling. *Mol. Cell. Proteomics* 10: M110.003335.
47. López-Ferrer, D., S. Martínez-Bartolomé, M. Villar, M. Campillos, F. Martín-Maroto, and J. Vázquez. 2004. Statistical model for large-scale peptide identification in databases from tandem mass spectra using SEQUEST. *Anal. Chem.* 76: 6853–6860.
48. Jorge, I., P. Navarro, P. Martínez-Acedo, E. Núñez, H. Serrano, A. Alfranca, J. M. Redondo, and J. Vázquez. 2009. Statistical model to analyze quantitative proteomics data obtained by 18O/16O labeling and linear ion trap mass spectrometry: application to the study of vascular endothelial growth factor-induced angiogenesis in endothelial cells. *Mol. Cell. Proteomics* 8: 1130–1149.
49. Martínez-Bartolomé, S., P. Navarro, F. Martín-Maroto, D. López-Ferrer, A. Ramos-Fernández, M. Villar, J. P. García-Ruiz, and J. Vázquez. 2008. Properties of average score distributions of SEQUEST: the probability ratio method. *Mol. Cell. Proteomics* 7: 1135–1145.

50. Navarro, P., and J. Vázquez. 2009. A refined method to calculate false discovery rates for peptide identification using decoy databases. *J. Proteome Res.* 8: 1792–1796.
51. Inokuchi, S., and J. B. Imboden. 1990. Antigen receptor-mediated regulation of sustained polyphosphoinositide turnover in a human T cell line. Evidence for a receptor-regulated pathway for production of phosphatidylinositol 4,5-bisphosphate. *J. Biol. Chem.* 265: 5983–5989.
52. Yin, H. L., and P. A. Janmey. 2003. Phosphoinositide regulation of the actin cytoskeleton. *Annu. Rev. Physiol.* 65: 761–789.
53. Haller, C., and O. T. Fackler. 2008. HIV-1 at the immunological and T-lymphocytic virological synapse. *Biol. Chem.* 389: 1253–1260.
54. Weng, J., D. N. Krementsov, S. Khurana, N. H. Roy, and M. Thali. 2009. Formation of syncytia is repressed by tetraspanins in human immunodeficiency virus type 1-producing cells. *J. Virol.* 83: 7467–7474.
55. Krementsov, D. N., J. Weng, M. Lambelé, N. H. Roy, and M. Thali. 2009. Tetraspanins regulate cell-to-cell transmission of HIV-1. *Retrovirology* 6: 64.
56. Irvine, D. J., M. A. Purbhoo, M. Krogsgaard, and M. M. Davis. 2002. Direct observation of ligand recognition by T cells. *Nature* 419: 845–849.
57. Beemiller, P., and M. F. Krummel. 2010. Mediation of T-cell activation by actin meshworks. *Cold Spring Harb. Perspect. Biol.* 2: a002444.
58. Douglass, A. D., and R. D. Vale. 2005. Single-molecule microscopy reveals plasma membrane microdomains created by protein-protein networks that exclude or trap signaling molecules in T cells. *Cell* 121: 937–950.
59. Imai, T., and O. Yoshie. 1993. C33 antigen and M38 antigen recognized by monoclonal antibodies inhibitory to syncytium formation by human T cell leukemia virus type 1 are both members of the transmembrane 4 superfamily and associate with each other and with CD4 or CD8 in T cells. *J. Immunol.* 151: 6470–6481.
60. Hayashi, K., and A. Altman. 2006. Filamin A is required for T cell activation mediated by protein kinase C-theta. *J. Immunol.* 177: 1721–1728.
61. Lasserre, R., S. Charrin, C. Cuche, A. Danckaert, M. I. Thoulouze, F. de Chaumont, T. Duong, N. Perrault, N. Varin-Blank, J. C. Olivo-Marin, et al. 2010. Ezrin tunes T-cell activation by controlling Dlg1 and microtubule positioning at the immunological synapse. *EMBO J.* 29: 2301–2314.
62. Barda-Saad, M., A. Braiman, R. Titerence, S. C. Bunnell, V. A. Barr, and L. E. Samelson. 2005. Dynamic molecular interactions linking the T cell antigen receptor to the actin cytoskeleton. *Nat. Immunol.* 6: 80–89.
63. Ilani, T., G. Vasiliver-Shamis, S. Vardhana, A. Bretscher, and M. L. Dustin. 2009. T cell antigen receptor signaling and immunological synapse stability require myosin IIA. *Nat. Immunol.* 10: 531–539.
64. Billadeau, D. D., J. C. Nolz, and T. S. Gomez. 2007. Regulation of T-cell activation by the cytoskeleton. *Nat. Rev. Immunol.* 7: 131–143.
65. Martín-Cófreces, N. B., J. Robles-Valero, J. R. Cabrero, M. Mittelbrunn, M. Gordón-Alonso, C. H. Sung, B. Alarcón, J. Vázquez, and F. Sánchez-Madrid. 2008. MTOC translocation modulates IS formation and controls sustained T cell signaling. *J. Cell Biol.* 182: 951–962.
66. Yoder, A., D. Yu, L. Dong, S. R. Iyer, X. Xu, J. Kelly, J. Liu, W. Wang, P. J. Vorster, L. Agulto, et al. 2008. HIV envelope-CXCR4 signaling activates cofilin to overcome cortical actin restriction in resting CD4 T cells. *Cell* 134: 782–792.
67. Campbell, E. M., R. Nunez, and T. J. Hope. 2004. Disruption of the actin cytoskeleton can complement the ability of Nef to enhance human immunodeficiency virus type 1 infectivity. *J. Virol.* 78: 5745–5755.
68. Iyengar, S., J. E. Hildreth, and D. H. Schwartz. 1998. Actin-dependent receptor colocalization required for human immunodeficiency virus entry into host cells. *J. Virol.* 72: 5251–5255.
69. Barrero-Villar, M., J. Barroso-González, J. R. Cabrero, M. Gordón-Alonso, S. Alvarez-Losada, M. A. Muñoz-Fernández, F. Sánchez-Madrid, and A. Valenzuela-Fernández. 2008. PI4P5-kinase Ialpha is required for efficient HIV-1 entry and infection of T cells. *J. Immunol.* 181: 6882–6888.
70. Corgan, A. M., C. Singleton, C. B. Santoso, and J. A. Greenwood. 2004. Phosphoinositides differentially regulate alpha-actinin flexibility and function. *Biochem. J.* 378: 1067–1072.
71. Barrero-Villar, M., J. R. Cabrero, M. Gordón-Alonso, J. Barroso-González, S. Alvarez-Losada, M. A. Muñoz-Fernández, F. Sánchez-Madrid, and A. Valenzuela-Fernández. 2009. Moesin is required for HIV-1-induced CD4-CXCR4 interaction, F-actin redistribution, membrane fusion and viral infection in lymphocytes. *J. Cell Sci.* 122: 103–113.